Journal of Engineering Physics and Thermophysics, Vol. 72, No. 6, 1999

INTEGRAL TRANSFER OF RADIATION OF THE ACTUAL SPECTRUM IN PROBLEMS OF RADIATIVE PLASMADYNAMICS

K. L. Stepanov, L. N. Panasenko,
G. S. Romanov, Yu. A. Stankevich, and
L. K. Stanchits

UDC 536.23:539.16

Radiative energy transfer in plasma is investigated with account for its actual optical properties. Consideration is based on the spectrum-integral method of partial characteristics. Databanks on integral partial characteristics of a number of substances are composed on the basis of data on optical properties that include the molecular state of matter, weakly ionized plasma, and plasma with multicharge ions and the main processes that determine absorption of thermal radiation (bound-bound, free-free, and bound-free transitions in molecules, atoms, and ions). Calculations of plasma radiation by this method are compared with results of spectral description. Some generalizations of the given method for solving problems of radiative plasmadynamics are considered.

Introduction. Inclusion of radiation greatly complicates solution of problems of high-temperature gasdynamics [1, 2]. A radiation flow and its divergence are spectrum-integral and angular-variable quantities that depend on the distribution of the parameters (temperature, density) in the entire volume under consideration. They should be determined rapidly and with sufficient accuracy on each time layer. It is obvious that direct integration over the spectrum in solving a gasdynamic problem is not used due to its laboriousness. The multigroup approximation, frequently used for simplification of calculations, where the actual spectrum is replaced by several tens of spectral groups within the limits of which the coefficients of absorption are averaged by one or another method (Rosseland methods or Planck mean-group methods, etc.), though giving a qualitatively accurate result, may greatly differ quantitatively from an approximation allowing for the actual spectrum. In particular, in [3] it is shown that under conditions where the radiative heat transfer is close to the limit of radiative thermal conductivity, the flow calculated in the multigroup approximation is severalfold lower than the actual one. We should distinguish a method of transfer calculation developed in [4] and based on averaging of the coefficients of absorption in groups over the field of intrinsic radiation with account for the actual spectral intensity and the diagram of radiation direction. The latter characteristics are found at individual instants of time (instants of averaging) and then are frozen along certain variables pertinent to each specific physical problem.

In the present paper, we used the spectrum-integral method of partial characteristics, which was developed in [5, 6], to describe radiation transfer in an actual spectrum. The method is based on representation of the radiation flow (for a plane layer) or the intensity in a prescribed direction (for an arbitrary geometry of the plasma) and their divergence in terms of spectrum-integral quantities. A databank of partial characteristics is composed for air, silicon dioxide, carbon dioxide, hydrogen, carbon, and aluminum, detailed test calculations are made, and possible ways of accelerating the calculation of the radiation field are studied.

Optical Properties of Plasma. To describe radiative transfer of energy we need data on the optical properties of matter. In the state of local thermal equilibrium they were calculated with account for the main radiative processes characteristic of hot gases and plasma. At temperatures $T \leq 10^4$ K, among these are absorption of radiation in electron-vibrational transitions in molecules and molecular ions, discrete transitions in atoms and ions, processes

Academic Scientific Complex "A. V. Luikov Heat and Mass Transfer Institute," National Academy of Sciences of Belarus, Minsk, Belarus. Translated from Inzhenerno-Fizicheskii Zhurnal, Vol. 72, No. 6, pp. 1103-1112. November–December, 1999. Original article submitted May 6, 1999.

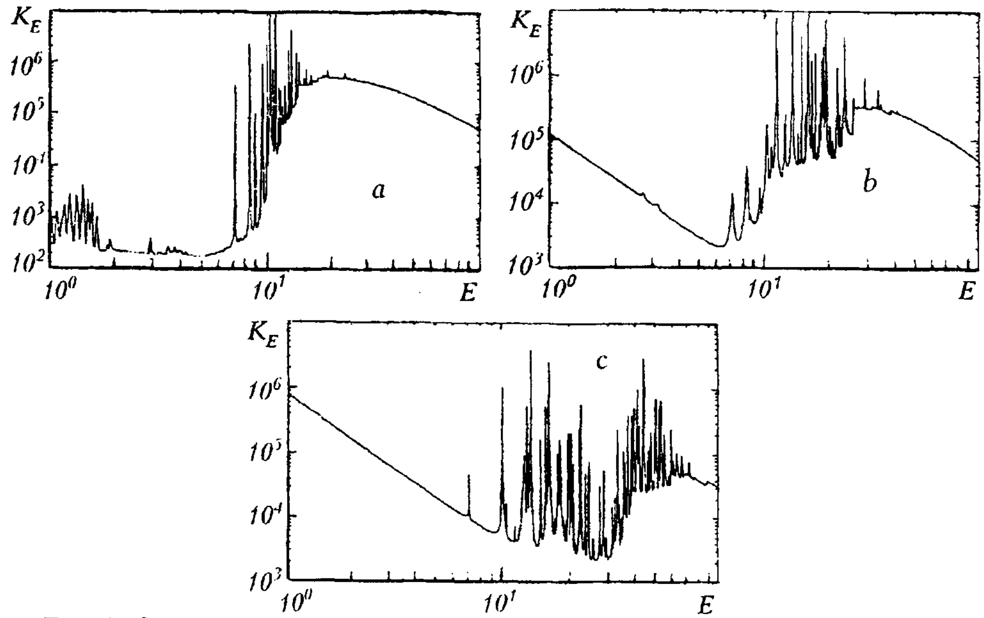

Fig. 1. Spectral mass coefficient of absorption of air with a density $\rho = 1.29 \cdot 10^{-3}$ g/cm^3 and a temperature $T = 1.02$ eV (a), 3.16 (b), and 10 (c). K_E, cm^2/g; E, eV.

of photodissociation and photoionization of molecules, and free-free transitions in the fields of neutral particles and ions. As the temperature increases, discrete transitions in atoms and ions, processes of photoionization of ground and excited levels and internal electron shells, and bremsstrahlung absorption in the fields of ions become predominant. A variety of radiative transitions, whose contribution to the total absorption changes sharply depending on the parameters of the plasma and the quantum energy, lead to a complex structure of the actual spectrum, which should be taken into account in solving problems of radiation transfer. In particular, radiation in spectral lines, in spite of their small width, can, in a number of cases, determine the magnitude of the radiation flow. This results in the need to describe the spectrum of the coefficient of absorption in detail.

We enumerate the main approximations adopted in calculations of coefficients of absorption of matter. The absorption cross section in free-free transitions in the fields of neutral particles was expressed in terms of the cross section of elastic scattering of an electron on this particle [7-9]. The absorption cross section in electron scattering on an ion was described by the Kramers formula with the Gaunt correcting multiplier [10]. Cross sections of bound-free transitions were calculated in various approximations. Photoionization of low-lying levels of atoms and ions of nitrogen and oxygen were calculated by the Hartree–Fock method [11]. Photoabsorption by other particles was determined by the quantum-defect method [12]. Cross sections of photoionization of hydrogen-like ions were calculated using exact formulas of the nonrelativistic dipole approximation [13]. Photoionization of excited levels was calculated in the quasiclassical approximation. The Hartree–Fock–Slater method was used for determination of photoionization cross sections of internal electron shells of atoms and ions [14]. Stepwise models [15] and data obtained under atmospheric conditions [16] were used for cross sections of photoionization of molecules. In calculation of absorption in spectral lines, their contour was prescribed in the form of a Voigt function that allows for collisional and thermal Doppler broadening. The linear Stark effect in the plasma microfield was taken into account for the hydrogen atom and H-like ions, and the line contour was specified according to Griem [17]. Absorption in electron-vibrational transitions of diatomic molecules was specified by an expression for the integral absorption in a band [18].

Coefficients of absorption of matter were calculated in the entire spectrum where transfer of intrinsic radiation is substantial ($E = 10^{-2}$–10^3 eV). The coefficients of absorption are averaged on rather small spectral ranges. The range of energies $E \leq 17.35$ eV contains, as in [19], 560 ranges of averaging with a step of 250 cm^{-1}, i.e., 0.03099 eV. In the harder range of the spectrum the step of averaging increases according to the law

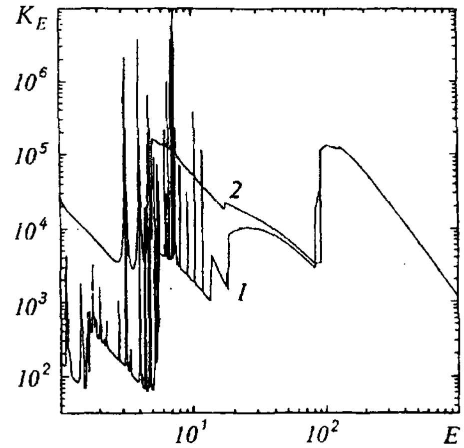

Fig. 2. Coefficient of absorption of aluminum plasma with $T = 1$ eV and $\rho = 1.21 \cdot 10^{-6}$ g/cm^3 (1) and $1.21 \cdot 10^{-4}$ (2).

$\Delta E_i = E_0 \cdot 10^{(i-560)/500}$ ($E_0 = 8.01 \cdot 10^{-2}$ eV). Thus, the total number of spectral ranges within the described range of energies of quanta is 1440.

Determination of the component composition of a plasma that is a complex mixture of molecules, atoms, and ions of different multiplicity of ionization is made by the "chemical model" [20]. Equilibrium concentrations for substances that have molecular components at temperatures $T \leq 10^4$ K are determined in accordance with the law of mass action for the leading components realized in the given temperature range. Molecular and atomic constants entering the equilibrium constants are contained in a databank on atomic characteristics of matter. The system of equations of chemical equilibrium in combination with the condition of quasineutrality and the equations of material balance is solved by relaxation methods [21].

When the molecular components are fully dissociated, the concentrations of ions of successive multiplicity of ionization are determined by the Saha system of equations. Here nonideality of the plasma is taken into account in terms of corrections to the ionization potentials obtained in the Debye annular approximation in a large canonical ensemble [22]. Planck–Larkin weighting functions [23] that reduce the contribution of highly excited states are introduced in calculation of statistical sums of particles.

Basic information on composed databanks of opticophysical characteristics of matter is given in [11, 21, 24-29]. The databank on optical properties of matter contains a set of tables of mass coefficients of absorption $K_E(T, \rho) = \kappa_E(T, \rho)/\rho$ (cm^2/g) as a function of the energy of the quanta, the temperature, and the density. Mass coefficients of absorption depend much more weakly on the density than linear ones, which increases the accuracy of interpolation of the tables to the required values of the parameters of the substance. Figure 1 presents the spectral mass coefficient of absorption of air at three temperatures as an example illustrating the obtained data. Figure 2 shows absorption of aluminum plasma.

Method of Partial Characteristics and a Databank for Its Application. The formal solution of the equation of radiation transfer on a ray of length L in the absence of sources on the boundaries is determined by the expression

$$I(x) = \int_0^\infty \int_0^L I_{E\mathrm{eq}}(\xi)\, \kappa_E(\xi) \exp\left(-\left|\int_\xi^x \kappa_E(y)\, dy\right|\right) \mathrm{sign}(x-\xi)\, dE\, d\xi . \tag{1}$$

The derivative of the intensity in the x direction is

$$\nabla I(x) = 2\int_0^\infty I_{E\mathrm{eq}}(x)\, \kappa_E(x)\, dE - \int_0^\infty \int_0^L I_{E\mathrm{eq}}(\xi)\, \kappa_E(\xi)\, \kappa_E(x) \exp\left(-\left|\int_\xi^x \kappa_E(y)\, dy\right|\right) dE\, d\xi . \tag{2}$$

Changing the order of integration in (1) and (2), after simple transformations [6] we can represent the corresponding expressions in the form

$$I(x) = \int_0^L \Delta I(\xi, x)\, \text{sign}(x - \xi)\, d\xi\,,$$

$$\nabla I(x) = \Delta I(x, 0) + \Delta I(x, L) - \int_0^L \Delta I_{\text{im}}(\xi, x)\, d\xi\,, \tag{3}$$

where the partial intensity $\Delta I(\xi, x)$ and the partial sink $\Delta I_{\text{im}}(\xi, x)$ are

$$\Delta I(\xi, x) = \int_0^\infty I_{E\text{eq}}(\xi)\, \kappa_E(\xi) \exp\left(-\left|\int_\xi^x \kappa_E(y)\, dy\right|\right) dE\,, \tag{4}$$

$$\Delta I_{\text{im}}(\xi, x) = \int_0^\infty [I_{E\text{eq}}(\xi) - I_{E\text{eq}}(x)]\, \kappa_E(\xi)\, \kappa_E(x) \exp\left(-\left|\int_\xi^x \kappa_E(y)\, dy\right|\right) dE\,. \tag{5}$$

Similarly, for a plane layer we found the radiation flow and its divergence:

$$S(x) = \int_0^L \Delta S(\xi, x)\, \text{sign}(x - \xi)\, d\xi\,,$$

$$\nabla S(x) = \Delta S(x, 0) + \Delta S(x, L) - \int_0^L \Delta S_{\text{im}}(\xi, x)\, d\xi\,, \tag{6}$$

$$\Delta S(\xi, x) = 2\int_0^\infty S_{E\text{eq}}(\xi)\, \kappa_E(\xi)\, E_2\left(\left|\int_\xi^x \kappa_E(y)\, dy\right|\right) dE\,, \tag{7}$$

$$\Delta S_{\text{im}}(\xi, x) = \int_0^\infty [S_{E\text{eq}}(\xi) - S_{E\text{eq}}(x)]\, \kappa_E(\xi)\, \kappa_E(x)\, E_1\left(\left|\int_\xi^x \kappa_E(y)\, dy\right|\right) dE\,. \tag{8}$$

Partial characteristics (4), (5) and (7), (8) can be calculated if the temperature and density (pressure) profile between the points ξ and x is specified and the spectral coefficient of absorption $\kappa_E(T, \rho)$ is known. The quantity $\Delta I(\xi, x)$ is, for example, determined by the distribution of the parameters along the ray in terms of the equilibrium intensity of the radiation $I_{E\text{eq}}(\xi)$ (this relation is local) and in terms of the optical distance $\tau_E = \int_\xi^x \kappa_E(y) dy$ between the points of radiation ξ and observation x. Since the dependence of τ_E on the spatial distribution of the thermodynamic variables has a character that is integral over the ray length and thus it is insensitive to the details of the profile of T and ρ between the points ξ and x, the possibility of integration over the energy of the quanta using splines that approximate the actual spatial dependences $T(y)$, $\rho(y)$ arises. The linear spline

$$T = T_x + (T_\xi - T_x)\, z\,, \quad \rho = \rho_x + (\rho_\xi - \rho_x)\, z\,, \quad z = \frac{y}{|\xi - x|}\,, \quad 0 \le z \le 1 \tag{9}$$

is the simplest. In this case, the tables of partial characteristics are five-dimensional (e.g., $\Delta S(\xi, x) = \Delta S(T_\xi, T_x, \rho_\xi, \rho_x, X)$). Linear splines provide the asymptotically correct behavior of the solution of the transfer equation in the limits of small and large optical thicknesses. For a transparent medium, where $\tau_E << 1$ in the whole range of the spectrum, the result is correct due to the absence of attenuation, and the distribution of radiation sources is always calculated on the true profile of the parameters T and ρ. In the opposite case ($\tau_E >> 1$), the intensity of the radiation $I(x)$ (or the flow) is determined by a small neighborhood of the point x, and here the linear approximation is usually quite sufficient.

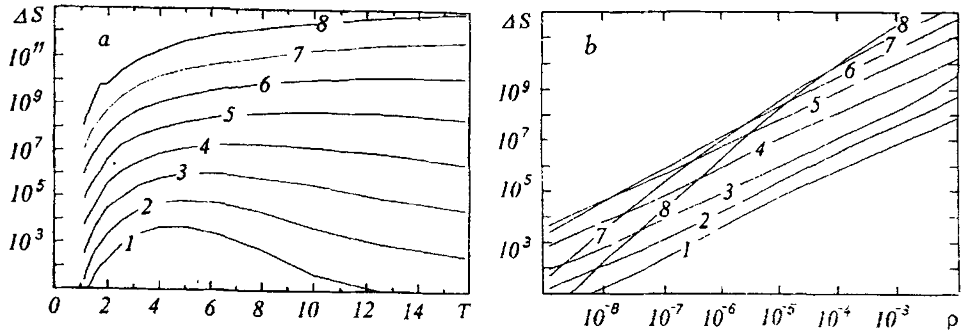

Fig. 3. Dependence of the partial flow on the temperature of the source (a): 1) $\rho = 10^{-9}$ g/cm^3; 2) 10^{-8}; 3) 10^{-7}; 4) 10^{-6}; 5) 10^{-5}; 6) 10^{-4}; 7) 10^{-3}; 8) 10^{-2} and its density (b): 1) $T = 1.3 \cdot 10^4$ K; 2) $1.6 \cdot 10^4$; 3) $2 \cdot 10^4$; 4) 2.51 eV; 5) 3.98; 6) 6.31; 7) 10; 8) 15.8. ΔS, W/cm^3; T, 10^3 K.

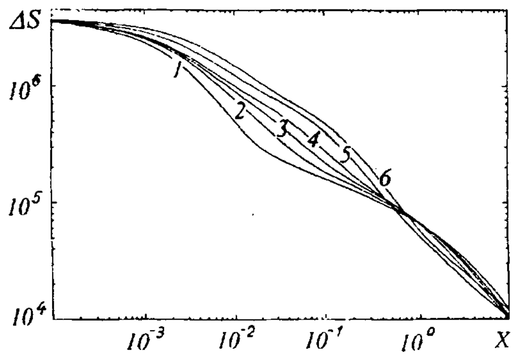

Fig. 4. Dependence of the partial flow on the distance for various temperatures of the sink: 1) $T_x = 2$ eV; 2) 1.85; 3) 1.72; 4) 1.55; 5) 1.20; 6) 0.34. $T_\xi = 2$ eV; $\rho_\xi = \rho_x = 1.29 \cdot 10^{-5}$ g/cm^3. X, cm.

Partial characteristics of plasma were calculated and tabulated in the approximation of linear splines in the same range of the parameters of state as the coefficients of absorption [28-30]. When $T < 2 \cdot 10^4$ K, the temperature scale of [19] (18 isotherms) was used, and when $T > 2 \cdot 10^4$ K a logarithmic step with $\Delta \log T = 0.1$ was specified. The density of the step was two points per order of magnitude. The range of temperatures was $10^3 \le T \le 10^6$ K, and the range of densities was $10^{-9} \le \rho \le 10^{-2}$ g/cm^3. The spatial range $X = |x - \xi|$ was tabulated with a frequency of 10 points per order of magnitude for $X = 10^{-4}$–10^5 cm. We note that the partial characteristics of air, hydrogen, and argon in [6] are given as a function of T, ρ, and X in rather narrow ranges of the parameters and are intended mainly for description of radiative transfer in laboratory set-ups for low-temperature plasma.

In composing tables of partial characteristics one should calculate the optical thickness $\int_\xi^x \kappa_E(y)dy$ between the point of the source and the point of observation accurately. For this it was assumed that on the portion of the path lying within the limits of the four nodes of the table of optical properties ($T_i \rho_j$, $T_i \rho_{j+1}$, $T_{i+1}\rho_j$, $T_{i+1}\rho_{j+1}$) the mass coefficient of absorption K_E can be represented in the form

$$\ln K = \ln K_1 + (\ln K_2 - \ln K_1) \frac{z - z_1}{z_2 - z_1}, \tag{10}$$

where K_1 and K_2 are the corresponding coefficients at the points of intersection of the ray with the boundaries of the given rectangle, and $z_2 - z_1$ is the portion of the path $X = |x - \xi|$ in it. Then the optical path between the points ξ and x is

$$\int_\xi^x \kappa\, dy = (x - \xi) \sum_i K_i \frac{z_{i+1} - z_i}{\ln\left(\frac{K_{i+1}}{K_i}\right)} \left\{ \frac{K_{i+1}}{K_i} \left[\rho_{i+1} - \frac{\rho_{i+1} - \rho_i}{\ln\left(\frac{K_{i+1}}{K_i}\right)}\right] - \left[\rho_i - \frac{\rho_{i+1} - \rho_i}{\ln\left(\frac{K_{i+1}}{K_i}\right)}\right]\right\}. \tag{11}$$

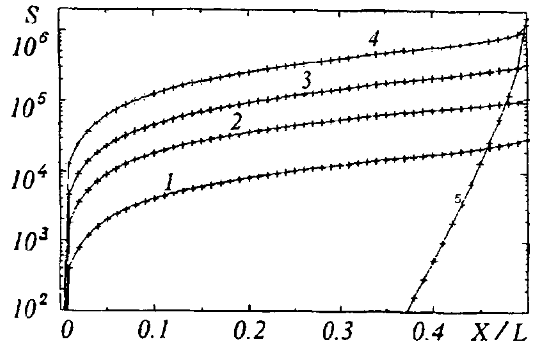

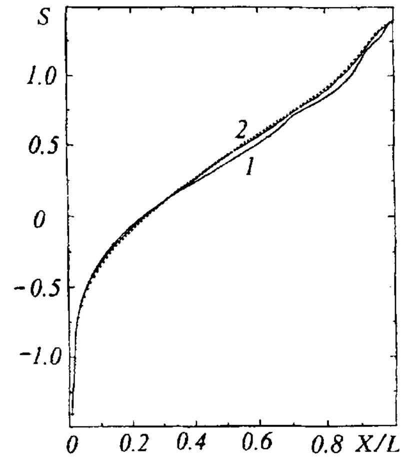

Fig. 5. Profile of the radiation flow in a uniform plane layer of the thickness L ($X = 0$ is the symmetry plane, $T = 2$ eV, $\rho = 1.29 \cdot 10^{-5}$ g/cm^3): 1) $L = 10^{-1}$ cm; 2) 10^0; 3) 10^1; 4) 10^3; 5) 10^5. S, W/cm^2.

Fig. 6. Radiation flow in an isothermal layer with a linear distribution of density ($T = 2$ eV, $L = 1$ cm, ρ (g/cm^3) $= 1.29 \cdot 10^{-3} - 1.28 \cdot 10^{-3} X/L$; crosses – spectral calculation): 1) in the table of partial characteristics the step in density is two points per order of magnitude; 2) four points per order of magnitude. S, MW/cm^2.

The contribution of an element of the table with a constant mass coefficient of absorption to the optical path is $(x - \xi)K_i(z_{i+1} - z_i)(\rho_i + \rho_{i+1})/2$.

Some results of calculation of partial characteristics of air are given in Fig. 3, where the dependence of ΔS on the temperature and density of the source is shown. We note that, since in these figures $X = 0$ ($\xi = x$), the partial flow turns out to be equal to $\Delta S(\xi, \xi) = 2\sigma T_\xi^4 \kappa_P$. Figure 4 shows the partial flow $\Delta S(\xi, x)$ in plasma with a constant density and a temperature of the source $T_\xi = 2$ eV, and the temperature of the point x is varied within the range $T_x = 2–0.34$ eV. It follows from the figure that the contribution of the point ξ to the flow $S(x)$ for a layer with a constant temperature of 2 eV at distances $X \le 1$ cm is smaller than in the case of lower temperatures T_x. This is caused by an increase in the transparency of the layer for radiation with a temperature $T_\xi = 2$ eV with decrease in the temperature T_x. For large distances this relation changes, which is associated with the postulate of linearity of the profiles of temperature and density between the points ξ and x and with the change in the relation between the spectrum-integral optical paths. At the same time, the value itself of this contribution decreases sharply with increase in the distance.

We note that radiative transfer under conditions where the spatial gradients of the pressure are small is much more convenient to calculate using temperature and pressure as independent parameters. In this case, due to the constancy of one of them (p = const) the tables of partial characteristics turn to be more compact. By virtue of the said above, they were also calculated as functions of the variables of T and p.

Results of Calculation of Radiative Transfer. To check the operation of the method we conducted a series of calculations of radiation of air plasma with various distributions of temperature and density (pressure). The data obtained were compared to results of spectral calculations where the transfer equation was solved on 1440 spectral ranges. Figure 5 demonstrates a profile of radiation flow in a plane layer with uniform distribution of the parameters. The dimensions of the layer vary within the range $10^{-1}-10^5$ cm. The integral calculation is shown by the solid curves, and the spectral one by the crosses. Complete graphical coincidence of the results obtained is seen. In calculation of radiation of a layer with a linear profile of temperature (the temperature of the left boundary is $T_0 = 2$ eV, and that of the right boundary is $T_1 = 0.862$ eV), a constant density $\rho = 1.29 \cdot 10^{-5}$ g/cm^3, and a characteristic size $10^{-1} < L < 10^2$ cm it turned out that the maximum differences observed for $L = 10^{-1}$ cm do not exceed 10%. An analysis shows that the differences are caused by the fact that in solving the spectral equations of transfer, interpolation between points of the table of optical properties is done for each energy of the quantum, whereas in the integral method it is done only once. It is apparent that to obtain a higher accuracy of the method of partial characteristics one should tabulate the corresponding data in greater detail. This is confirmed by the results presented in Fig. 6, where a profile of the flow in an isothermal layer with a linear profile of density is shown, and its difference on the boundaries of the layer is two orders of magnitude. It is seen that use of more detailed tables (four points per order of magnitude in ρ) gives better correspondence to spectral data.

We next consider radiation of a plasma layer with a nonlinear distribution of temperature. Let the profile of T have the form

$$T(x) = \frac{T_0}{1 + A(x/L)^{\alpha}}, \quad A = \frac{T_0}{T_1} - 1. \tag{12}$$

We calculated two versions of relation (12): with $\alpha = 2$ and 5. The density was assumed constant and equal to $1.29 \cdot 10^{-5}$ g/cm^3, and the dimensions of the layer were varied. On the left boundary $T_0 = 2$ eV, on the right $T_1 = 0.862$ eV, and the layer thickness is $L = 10^{-1} - 10^3$ cm. A comparison of the profile of the radiation flow obtained by the spectral method (crosses) and by the integral method (the dashed curve) is given in Fig. 7. Since the temperature profile with $\alpha = 2$ is noticeably closer to linear, better correspondence to spectral results is observed for it. As L increases (as the gradients decrease and the nontransparency of the layer increases), the integral results approach the spectral ones.

In using linear splines, besides the actual temperature at the point x, as was done in all previous calculations, we can select as T_x the temperature T'_x that provides the best approximation of a linear profile on the path of absorption to the actual one [5]. From obvious considerations, the effective temperature of the point T'_x and the effective density at it are determined by a distribution of T and ρ between the points ξ and x such that the total integral of the actual distribution is equal to the integral of the linear profile:

$$\int_{\xi}^{x} T(y)\, dy = \frac{1}{2}(T_{\xi} + T'_x)(x - \xi), \quad \int_{\xi}^{x} \rho(y)\, dy = \frac{1}{2}(\rho_{\xi} + \rho'_x)(x - \xi). \tag{13}$$

For profile (12) with the parameter $\alpha = 2$ the effective temperature is

$$T'_x(\xi, x) = \frac{2T_0 L}{\sqrt{A}} \left\{ \arctan \frac{x\sqrt{A}}{L} - \arctan \frac{\xi\sqrt{A}}{L} \right\} (x - \xi)^{-1} - T_{\xi}. \tag{14}$$

With $\alpha = 5$ we have for T'_x

$$T'_x(\xi, x) = \frac{2T_0 L}{A^{\beta}} \times$$

$$\times \left\{ \beta \ln |z + 1| - \beta \sum_{k=0}^{1} \cos[\beta(2k + 1)\pi] \ln[z^2 - 2z\cos[\beta(2k + 1)\pi] + 1] + \right.$$

$$\left. + 2\beta \sum_{k=0}^{1} \sin[\beta(2k + 1)\pi] \arctan \frac{z - \cos[\beta(2k + 1)\pi]}{\sin[\beta(2k + 1)\pi]} \right\}_{\frac{\xi A^{\beta}}{L}}^{\frac{xA^{\beta}}{L}} (x - \xi)^{-1} - T_{\xi}, \tag{15}$$

where $\beta = 1/\alpha = 0.2$. The calculation of the flow with the effective temperature T'_x according to (14), (15) is presented in Fig. 7 (curves 3). It is seen from the figure that introduction of the effective temperature T'_x refines the data of the integral method in the requisite direction. The value of T'_x can differ noticeably from T_x. If $T'_x > T_x$, this means that on a large part of the path of absorption the actual temperature is higher than on the linear spline, and conversely, when $T'_x < T_x$, the temperature on the spline mainly exceeds the actual temperature. Therefore for the case $T'_x > T_x$, the partial flow $\Delta S(\xi, x)$ can be represented in the form of a combination of the

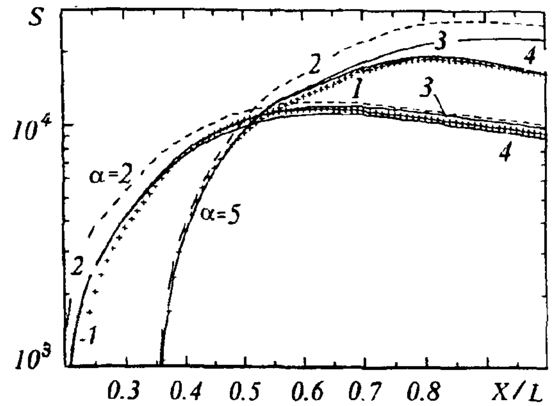

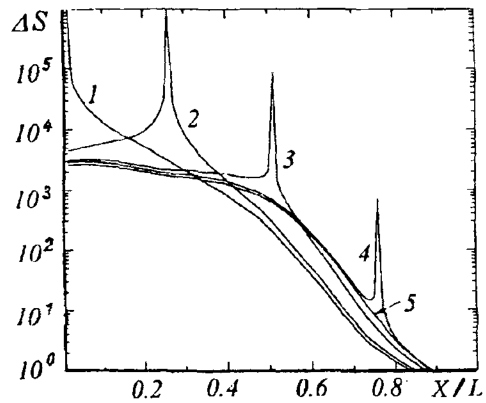

Fig. 7. Comparison of various approximations for describing a radiation flow by the method of partial characteristics ($L = 10^{-1}$ cm, $\rho = 1.29 \cdot 10^{-5}$ g/cm^3): 1) spectral calculation (crosses); 2) calculation with the local temperature T_x; 3) calculation with the temperature T_x' of (14), (15); 4) calculation with the partial flow of (16).

Fig. 8. Spatial distribution of partial flows in a plane layer of air plasma with $\rho = 1.29 \cdot 10^{-5}$ g/cm^3, $L = 10^2$ cm, the temperature profile of (12) with $\alpha = 2$, $T_0 = 2$ and $T_1 = 0.5$ eV: 1) $X/L = 0$; 2) 0.25; 3) 0.5; 4) 0.75; 5) 1.

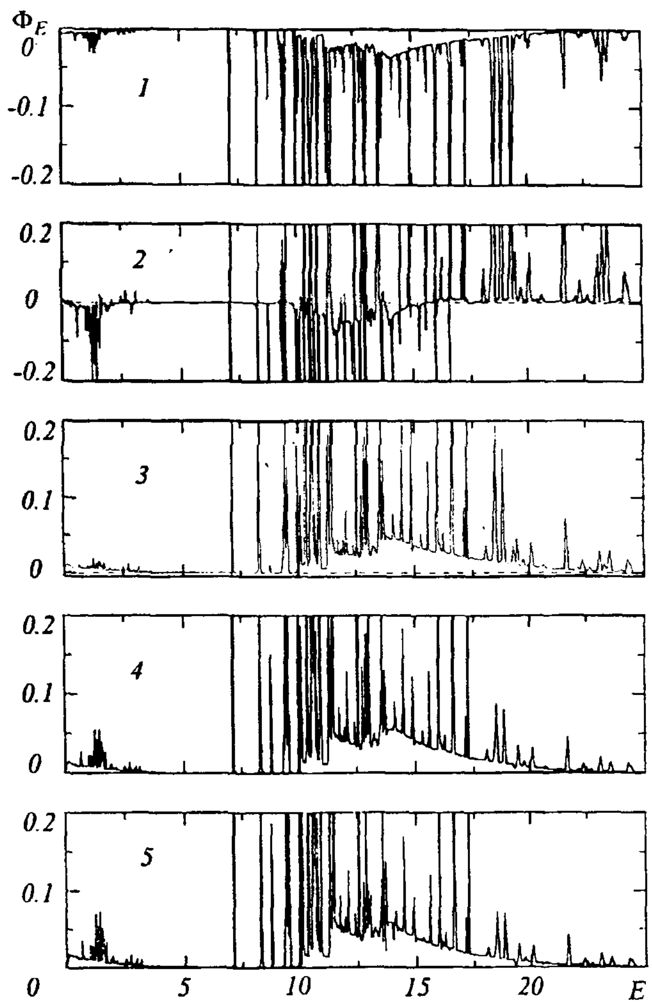

Fig. 9. Spectral function of flow in various cross sections of a plane layer of air plasma: 1) $X/L = 0$; 2) 0.25; 3) 0.5; 4) 0.75; 5) 1. Φ_E, eV^{-1}; E, eV.

partial flow $\Delta S(\xi, T_\xi; x, T_x')$ and a partial flow along an isothermal path $\Delta S(\xi, T_\xi; x, T_x)$ each weighted with a certain weight. Curves 4 in Fig. 7 correspond to this calculation. Here the partial flow is taken in the form

$$\Delta S(\xi, x) = \Delta S(T_\xi, T_x')(T_x/T_x')^3 + \Delta S(T_\xi, T_\xi)[1 - (T_x/T_x')^3]. \tag{16}$$

As is seen, this procedure provides a more correct behavior of the radiant flow in transparent layers with a high gradient of the temperature. Similar results for the intensity of the radiation of plasma arc of constant pressure in air are obtained in [30].

According to (3) and (6), intensities, flows, and their divergences are found by integration of partial characteristics over a ray (a layer). Because of possible nonmonotonic and sharp variation of the partial characteristics in space this problem is rather complicated. To solve it we can use quadrature formulas with a controllable accuracy. In the case of strong nontransparency of the plasma in the local vicinity of the point x, the partial intensities (flows) change by many orders of magnitude. Here the resultant flow is a small difference between large and close one-sided flows. In Fig. 8 the distribution of the partial flow is shown for five cross sections of a plane layer with a thickness $L = 10^2$ cm, constant ρ, and a profile of T according to (12). The radiative flow is equal to the difference between the areas under the corresponding curves on either side of the point x. An analysis showed that in this case the most effective way to calculate the radiation is to use tables containing partial characteristics integrated over a linear profile of the parameters (e.g., $\int_\xi^x \Delta S(\xi, x)d\xi = F(T_\xi, T_x, \rho_\xi, \rho_x, X)$). Clearly they can be used only in the local vicinity of the point x, where the linear approximation for the profile of T and ρ is justified.

The spectral parameters of the radiation give an idea about the complex character of radiative transfer in a plane layer of air plasma. Figure 9 demonstrates the spectral flow of radiation in various cross sections of a layer with the parameters $L = 10^{-1}$ cm, $T_0 = 2$ eV, $T_1 = 0.862$ eV; the temperature profile is specified according to (12), $\alpha = 2$, $\rho = 1.29 \cdot 10^{-5}$ g/cm^3. The graph shows the function describing the energy spectrum of the local radiative flow $\Phi_E = S_E/|S|$. It is normalized to unity and retains the sign of the spectral flow. We note that in the cross section $L/4$ spectral flows in various ranges of the spectrum have different directions. The sign of the flow depends on the distribution of the radiation sources and the optical thickness of the plasma on either side of the point of observation. Spectral flows are calculated using the flow scheme of the solution of the transfer equation [3].

Conclusion. The data presented show that in describing radiative transfer in the case where the actual spectrum is characterized by many hundreds of intense lines and recombination continua where the intensity changes by an order of magnitude, use of the method of partial characteristics with certain modifications provides rather high accuracy of the determination of integral flows and intensities of radiation. This gives hope that this method will be used successfully for solving problems of nonstationary radiation gasdynamics.

The work was carried out under the program of the International Science and Technology Center, project B23-96.

NOTATION

T, tempereture; ρ, density; p, pressure; S, flow of radiation energy; I, intensity of radiation; K_E, spectral mass coefficient of absorption; κ_E, linear coefficient of absorption; $I_{E_{eq}}$ and $S_{E_{eq}}$, equilibrium intensity and flow; E, quantum energy; ξ and x, spatial variables; ΔI and ΔS, partial intensity and flow; ΔI_{im} and ΔS_{im}, partial sinks of intensity and flow; E_1 and E_2, integral indicative functions of the 1st and 2nd kind; τ_E, optical thickness; $\bar{\kappa}_P$, Planck mean coefficient of absorption; L, characteristic linear dimension of the plasma; Φ_E, normalized spectral function of flow.

REFERENCES

1. D. M. Mihalas and B. W. Mihalas, *Foundations of Radiation Gasdynamics*, N. Y. (1984).

2. B. N. Chetverushkin, *Mathematical Simulation of Problems of the Dynamics of a Radiating Gas* [in Russian], Moscow (1985).
3. K. L. Stepanov, L. K. Stanchits, and Yu. A. Stankevich, *Structure of Radiating Strong Shock Waves Propagating in the Atmosphere of the Earth*, Preprint No. 2 of the Academic Scientific Complex "A. V. Luikov Heat and Mass Transfer Institute," National Academy of Sciences of Belarus [in Russian], Minsk (1998).
4. I. V. Nemchinov, *Prikl. Mat. Mekh.*, **34**, No. 4, 706-721 (1970).
5. V. G. Sevast'yanenko, *Radiative Heat Transfer in a Real Spectrum*, Dissertation for Doctor of Physical and Mathematical Sciences, Novosibirsk [in Russian] (1980).
6. R. I. Soloukhin (ed.), *Radiative Heat Transfer in High-Temperature Gases: Reference Book* [in Russian], Moscow (1984).
7. V. A. Kas'yanov and A. N. Starostin, *Zh. Éksp. Teor. Fiz.*, **48**, No. 1, 295-302 (1965).
8. O. B. Firsov and M. I. Chibisov, *Zh. Éksp. Teor. Fiz.*, 39, No. 6 (12), 1770-1776 (1960).
9. V. A. Kamenshchikov, Yu. A. Plastinin, and V. M. Nikolaev, *Radiative Properties of Gases at High Temperatures* [in Russian], Moscow (1971).
10. J. R. Stallop and K. W. Billman, *Plasma Phys.*, **16**, 1187-1189 (1974).
11. G. S. Romanov, Yu. A Stankevich, L. K. Stanchits, and K. L. Stepanov, *Thermodynamic Properties and Spectral and Mean Coefficients of Absorption of Multicomponent Gases in a Wide Range of the Parameters*, Preprint No. 2 of the Academic Scientific Complex "A. V. Luikov Heat and Mass Transfer Institute," National Academy of Sciences of Belarus [in Russian], Minsk (1993).
12. A. Burgess and M. J. Seaton, *Mon. Not. Roy. Astron. Soc.* **120**, No. 2, 121-151 (1960).
13. H. A. Bethe and E. E. Salpeter, *Quantum Mechanics of One- and Two-Electron Atoms*, Springer-Verlag (1957).
14. F. N. Borovik, G. S. Romanov, and K. L. Stepanov, *Cross Sections of Continuous Absorption of Multiply Ionized Plasma of Carbon*, Deposited at VINITI on 23.01.81, No. 4912-81 (1981).
15. I. T. Surzhikov, *Computational Experiment in Construction of Radiation Models of the Mechanics of a Radiating Gas* [in Russian], Moscow (1992).
16. K. Watanabe, in: *Study of the Upper Atmosphere by Rockets and Satellites* [Russian translation], Moscow (1961), pp. 280-358.
17. H. R. Griem, *Spectral Line Broadening by Plasma*, N. Y.–London (1974).
18. L. A. Kuznetsova, N. E. Kuz'menko, and Yu. Ya. Kuzyakov, *Probabilities of Optical Transitions of Diatomic Molecules* [in Russian], Moscow (1980).
19. I. V. Avilova, L. M. Biberman, V. S. Vorob'ev, et al., *Optical Properties of Hot Air* [in Russian], Moscow (1970).
20. V. K. Gryaznov, I. L. Iosilevskii, Yu. G. Krasnikov, et al., *Thermophysical Properties of the Working Media of a Gas-Phase Nuclear Reactor* [in Russian], Moscow (1980).
21. G. S. Romanov, Yu. A. Stankevich, L. K. Stanchits, and K. L. Stepanov, *Inzh.-Fiz. Zh.*, **68**, No. 2, 291-305 (1995).
22. A. A. Likal'ter, *Zh. Éksp. Teor. Fiz.*, **56**, No. 1, 240-245 (1969).
23. L. P. Kudrin, *Statistical Physics of Plasma* [in Russian], Moscow (1974).
24. S. I. Kas'kova, G. S. Romanov, K. L. Stepanov, and V. I. Tolkach, *Opt. Spektrosk.*, **45**, No. 4, 655-662 (1979).
25. G. S. Romanov, K. L. Stepanov, and M. I. Syrkin, *Opt. Spektrosk.*, **46**, No. 5, 860-868 (1979).
26. K. L. Stepanov, F. N. Borovik, S. I. Kas'kova, and G. S. Romanov, *Opt. Spektrosk.*, **52**, No. 4, 614-620 (1982).
27. G. S. Romanov, K. L. Stepanov, and M. I. Syrkin, *Opt. Spektrosk.*, **53**, No. 4, 642-648 (1982).
28. G. S. Romanov, Yu. A. Stankevich, L. K. Stanchits, and K. L. Stepanov, *Int. J. Heat Mass Transfer*, **38**, No. 3, 545-556 (1995).
29. K. L. Stepanov and L. K. Stanchits, *Zh. Prikl. Spektrosk.*, **65**, No. 1, 22-26 (1998).
30. K. L. Stepanov, E. A. Ershov-Pavlov, V. E. Okunev, et al., *Radiative Energy Transfer in Axisymmetric Electric Discharges and Plasma Jets*, Preprint No. 4 of the Academic Scientific Complex "A. V. Luikov Heat and Mass Transfer Institute," National Academy of Sciences of Belarus [in Russian], Minsk (1999).